Kinetic Gelation Modeling: Kinetics of Cross-Linking Polymerization

Mei Wen,† L. E. Scriven, and Alon V. McCormick*

Department of Chemical Engineering & Materials Science and Center for Interfacial Engineering, University of Minnesota, Minneapolis, Minnesota 55455

Received February 21, 2001; Revised Manuscript Received December 20, 2002

ABSTRACT: A kinetic gelation model that simulates free-radical network polymerization on a lattice with a stochastic kinetic approach to enable real time calculation was used to assess how initiation rate and primary cyclization affect the overall kinetics of polymerization of difunctional monomers. Changes that cause a more uniform distribution of reacted sites—higher initiation rate or less primary cyclization—increase the accessibility of free radicals to functional groups, lower the fraction of trapped radicals, and consequently raise the apparent propagation rate constant. On the other hand, the final conversion, determined by kinetic chain length at a given initiator concentration, drops when termination becomes more severe such as under higher initiation rate or when radical trapping worsens such as under enhanced cyclization. In addition, the model simulates the contribution of pendant functional groups to the formation of different structures. The higher the radical concentration brought by higher initiation rate or by less preferred primary cyclization, the lower the fraction of pendant functional groups to form primary cycles and the higher the fractions of pendant functional groups to form cross-links and secondary cycles.

Introduction

Photopolymerization of multifunctional monomers such as diacrylates forms highly cross-linked polymer networks.[1−4] The kinetics of cross-linking polymerization behaves anomalously (compared to linear polymerization) because diffusion of functional groups and free radicals quickly becomes severely limited; most notable is trapping of radicals[5,6] and severe reaction−diffusion.[7,8] Consequently, cross-linking polymerization kinetics is closely linked to the structure development of the network polymers formed. Under diffusion limitation, growing polymer chains quickly cyclize and cross-link into clusters (sometimes referred to as microgels), and the clusters are linked up into a sample-spanning network. The highly cross-linked clusters can trap radicals, shielding them from further polymerization, even at very low overall conversion. At high conversions, radicals can also become trapped by virtue of the substantially reduced mobility (vitrification) as microgel regions connect into a larger, ultimately sample-spanning, network.[6,9] At some point—early in reaction for highly cross-linking systems—ordinary diffusion becomes less important than reaction−diffusion (the motion of radicals only by propagating along their kinetic chains) to the overall kinetics. Furthermore, because radicals become trapped in highly reacted regions, spatial inhomogeneity—local variations in conversion so that more highly reacted regions coexist with less highly reacted region—comes to govern the populations of active and trapped radicals, the accessibility of free radicals to functional groups, and thus the overall kinetics. Because of the close relation between polymerization kinetics and the details of network growth, it is essential to study both of them in one model.

Two methods are generally used to simulate free-radical cross-linking polymerization. One is the mean-field kinetic modeling, in which reactions are presumed to occur uniformly throughout the system and a set of differential equations with apparent deterministic rate constants need to be solved. The other is the kinetic gelation modeling, which models network growth on a lattice. In general, mean-field kinetic modeling simulates polymerization kinetics with little network information except as imposed by empirical adjustments to apparent rate constants,[10−14] whereas kinetic gelation modeling explicitly takes into account network growth and conversion of functional groups—but often without real reaction time information.[15−20]

The approach to kinetic gelation modeling presented in the preceding paper (also referred to as part 1),[21] though, allows us to simulate more reasonably both the polymerization kinetics and network growth in one model. The model recasts polymerization kinetics as a Markov process through a stochastic approach. It simulates real reaction time by modifying and employing the probability density function and the associated Monte Carlo method devised originally by Gillespie[22] to reactions on a lattice.

In part 1,[21] the spatial distributions of reacted sites, doubly reacted sites, and unreacted sites were examined. It was found that either faster initiation or suppression of primary cyclization leads to a more homogeneous network structure, and these trends were quantified. In this work, the effects these trends have on overall polymerization kinetics are investigated. Various measures relating to these kinetics are monitored, including populations of active and trapped radicals, the accessibility of free radicals to functional groups, the apparent propagation rate constant, conversion profiles, kinetic chain length, and distributions of reacted pendant functional groups in primary cycles, secondary cycles, and cross-links.

Modeling Method

Full details of this model were described in part 1.[21] Presented here is a brief review of its most salient features.

A simple cubic lattice was employed; its sites were initially occupied by monomers and initiators. Reaction

† Present address: Atofina Chemicals, Inc., 900 First Ave., King of Prussia, PA 19406.

* To whom correspondence should be addressed.

10.1021/ma010309i CCC: $25.00 © 2003 American Chemical Society
Published on Web 05/07/2003

was allowed only between first-nearest neighbors. Reaction kinetics was simulated by using stochastic formulation, where the reaction rate constants were viewed not as reaction rates per unit time per unit volume but as reaction probabilities per unit time. For simplicity, explicit movements of monomers and polymers on the lattice were not represented, but local reactive site thermal motions of course were reflected in part in the reaction probabilities, which were themselves proportional to the stochastic reaction rate constants. The stochastic propagation rate constant k_p specified the propagation probability per unit time of a combination of a radical and a functional group that are not able to form a primary cycle. The "primary cyclization rate constant" was simply the stochastic propagation rate constant k_p multiplied by an adjustable enhancement factor r, enabling study of the choice of monomer with structure that might encourage attack by the radical on a pendant functional group that is on the same kinetic chain (backbiting). The termination rate constant k_t specified the termination probability per unit time of a combination of two radicals. These stochastic reaction rate constants were assumed to remain constant throughout polymerization. Both k_p and k_t were estimated from experimental values of the apparent deterministic rate constants at the beginning of polymerization.

Before a propagation or termination took place, the reaction probabilities of all the radicals reacting with their neighbors were calculated. A waiting time was then calculated from the summation of all the reaction probabilities according to a Monte Carlo technique.[22] Thereafter, a pair of reactive sites was chosen to react according to all the reaction probabilities. This process was repeated until no active radicals were present on the lattice.

During the stochastic propagation and termination process, initiation took place following a first-order, deterministic kinetics. The simulation was continued until initiators were exhausted; i.e., no more active (untrapped) radicals were present, and only one initiator was left (it would take an infinitely long time to decompose the last initiator). The conversion reached upon initiator exhaustion is defined as the final conversion here. It is important to note this definition—it does not necessarily correspond to various experimental definitions used.

From a simulated conversion profile, we could calculate how the apparent deterministic propagation rate constant (simply called apparent propagation rate constant below) k_p' changes as a function of conversion, an important parameter which is needed in the mean-field kinetic modeling and can be measured experimentally. This requires evaluating the slopes of the conversion profile at different conversions. Another simple way, which was used in this work, is to calculate k_p' through its correlation[21] to the stochastic propagation rate constant k_p

$$k_p' = \frac{\langle \overline{(N_M)_{rad}} \rangle}{[M_{tot}]} k_p \qquad (1)$$

where $[M_{tot}]$ is the total functional group concentration, $\langle \overline{(N_M)_{rad}} \rangle$ is the apparent average number of functional groups neighboring each radical (including both active and trapped), and $\langle \cdots \rangle$ (as omitted below) denotes the average taken over an ensemble of stochastically identical systems. Physically, when the primary cyclization rate factor $r = 1$ (primary cyclization is not preferred, but occurs randomly), $\overline{(N_M)_{rad}}$ is the actual average number of functional groups neighboring each radical $\overline{(N_M)^0_{rad}}$ in the simulation. However, when $r > 1$ (primary cyclization is preferred), $\overline{(N_M)_{rad}}$ is larger than $\overline{(N_M)^0_{rad}}$.

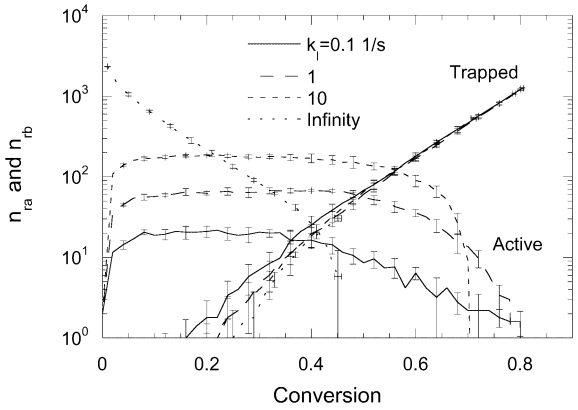

Figure 1. Effect of initiation rate constant k_I on the numbers of active n_{ra} and trapped n_{rb} radicals during polymerization. The vertical range bars of every other points are shown, which indicate plus or minus one standard deviation at a given conversion. At the end of each curve, the conversion is the mean final conversion, and the horizontal range bars there indicate plus or minus one standard deviation of the final conversion.

The actual average number of functional groups neighboring each radical $\overline{(N_M)^0_{rad}}$ serves as a measure of the accessibility of free radicals to functional groups on a lattice.

Simulations were run on a $50 \times 50 \times 50$ lattice with the same base-case simulation parameters as used in part 1.[21] Those parameters are initiator concentration = 1%, initiation rate constant $k_I = 1$ 1/s, propagation rate constant $k_p = 10^3$ 1/s, termination rate constant $k_t = 10^7$ 1/s, and primary cyclization enhancement factor $r = 1$. The average of five realizations was reported. Standard deviations are shown for only half of the data points to reduce clutter. Curves shown without standard deviations mean that the variance is smaller than the graphic shown.

Results and Discussion

Effect of Initiation Rate Constant. Figure 1 shows the numbers of active and trapped radicals vs the conversion of functional groups at different initiation rate constants k_I. At a finite k_I, the number of active radicals rises sharply at the beginning of the reaction. Then it grows further because termination is limited by reaction−diffusion on a lattice from the beginning of the reaction. After that it remains almost constant under the balance of generation of new radicals and termination of existing radicals. This pseudo-steady-state number of active radicals remains until radical trapping becomes dominant, where the number of trapped radicals surpasses the number of active radicals. Then the number of active radicals drops rapidly because of depletion of initiators and severe trapping of radicals. In contrast, trapped radicals appear around 0.2 conversion. Thereafter, the number of trapped radicals rises monotonically with conversion. This trend of active and trapped radicals agrees with experimental

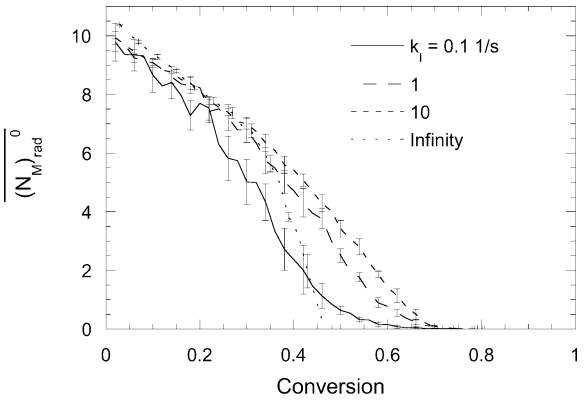

Figure 2. Effect of initiation rate constant k_I on the actual average number of functional groups neighboring each radical $\overline{(N_M)^0_{rad}}$. Range bars of every other points are shown, which indicate plus or minus one standard deviation at a given conversion.

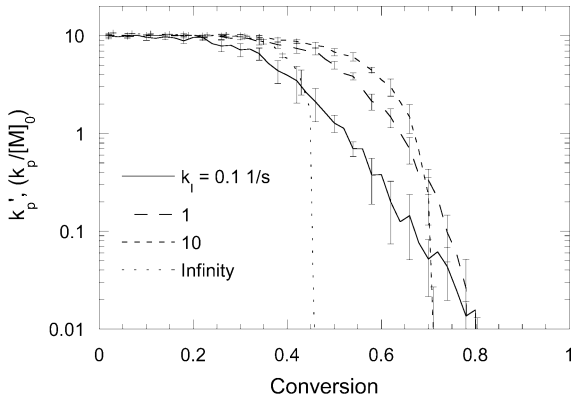

Figure 3. Effect of initiation rate constant k_I on the apparent propagation rate constant k_p'. Range bars of every other points are shown, which indicate plus or minus one standard deviation at a given conversion.

observation of the liquidlike (active) radicals and the solidlike (trapped) radicals obtained by electron spin resonance spectroscopy (ESR).[6] In the special case of $k_I = \infty$, wherein all the initiators decompose into radicals instantaneously, the number of active radicals monotonically decays because of termination and trapping.

When the initiation rate constant is raised, more active radicals are present throughout most of the reaction period. Late in the reaction, the number of active radicals starts to drop faster because most initiators have been depleted. The number of trapped radicals is not much affected by the initiation rate constant at a given conversion. Consequently, the higher the initiation rate constant, the lower the fraction of the number of trapped radicals over the number of all the radicals (including active and trapped) and the later the number of trapped radicals surpasses the number of active radicals. This trend agrees with the experiment observation in the photopolymerization of diethylene glycol dimethacrylate (DEGDMA).[6] The final number of trapped radicals (as initiators are exhausted) reaches a higher value as k_I drops because less radicals have been terminated.

Faster initiation leads to a more uniform distribution of reacted sites or a more homogeneous structure at a given conversion (see analysis in part 1[21]). Here it suggests that a more homogeneous structure lowers the fraction of trapped radicals, easing propagation.

The actual average number of functional groups neighboring each radical (Figure 2) and the apparent propagation rate constant (Figure 3) during reaction give further measures of the effect of structural inhomogeneity on polymerization kinetics.

The actual average number of functional groups neighboring each radical $\overline{(N_M)^0_{rad}}$ measures the accessibility of free radicals to functional groups. ($\overline{(N_M)^0_{rad}}$ starts at 10 when the first free radical is generated. This is $2(n - 1)$, where n is the lattice coordinate number, because initially the decomposed initiator that generates the free radical is also a neighbor of the free radical.) At low conversions, $\overline{(N_M)^0_{rad}}$ drops almost linearly. At different initiation rate constants, the curves overlay each other because the drop of $\overline{(N_M)^0_{rad}}$ is caused solely by depletion of functional groups. However, the curves depart from linearity—$\overline{(N_M)^0_{rad}}$ drops faster—at higher conversions. The departure is delayed to higher conversions (e.g., up to 0.22 conversion at $k_I = 0.1$ 1/s, 0.28 conversion at $k_I = 1$ 1/s, and 0.32 conversion at $k_I = 10$ 1/s), and the departure is less severe when the initiation rate constant is raised. Apparently, the more homogeneous structure maintains more reaction partners.

The apparent propagation rate constant k_p' in the units of $k_p/[M_0]$ shows about 3 orders of magnitude change during reaction. Consistent with the trend known in $\overline{(N_M)^0_{rad}}$, at low conversions, k_p' remains nearly constant, indicating that the propagation is not spatially controlled. Then k_p' starts to drop as conversion rises, indicating that propagation becomes more controlled by the availability of neighboring functional groups. Radicals are more and more buried and ultimately trapped in highly cross-linked regions. This trend of k_p' change has been observed in experimental studies.[7,23,24]

Increasing the initiation rate constant delays the drop in k_p' to a higher conversion. Figure 3 shows the first time that structural homogeneity (higher initiation rate constant) better maintains a high apparent propagation rate constant. The final rapid drop of k_p' is caused by both the depletion of initiators and active radicals. Clearly, there can be no meaningful measure of the apparent propagation rate constant or the actual number of functional groups neighboring each radical (accessibility) when there are no free radicals that can find functional groups in their neighbors. (With the instantaneous initiation at $k_I = \infty$, neither $\overline{(N_M)^0_{rad}}$ nor k_p' suggests any accessibility change before conversion reaches 0.35. After this conversion, they both drop rapidly because of the depletion of active radicals by severe termination of radicals.)

Figure 4 shows the conversion profiles at different initiation rate constants. Because of the large difference in reaction time at different initiation rate constants, the conversion profiles shown in Figure 4a do not include the whole reaction courses at $k_I = 0.1$ 1/s and $k_I = 1$ 1/s. To overcome this limitation, the conversion profiles are further presented in Figure 4b (not including $k_I = \infty$) by using a dimensionless time, the product of initiation rate constant and the reaction time. In agreement with experiment, the conversion profiles shown in Figure 4a are S-shaped. Initially the reaction rate is relatively low, then it rapidly rises, reaching a maximum rate, and finally it slows down. Because there is no explicit motion on the lattice, the termination of radicals is controlled from the beginning by reaction—

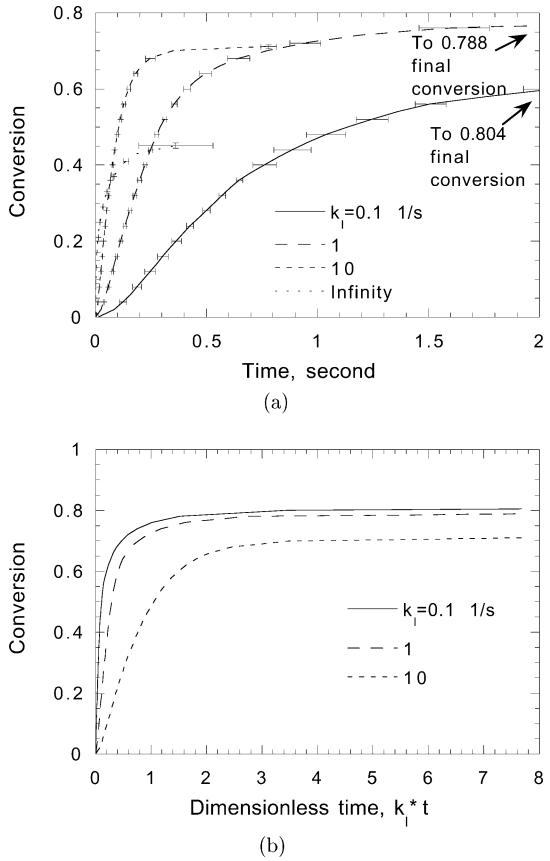

Figure 4. Effect of initiation rate constant k_I on the conversion profiles plotted in (a) time and (b) dimensionless time. The horizontal range bars of every other points are shown in (a), which indicate plus or minus one standard deviation at a given conversion. At the end points in (a), the conversion is the mean final conversion, and the vertical range bars indicate plus or minus one standard deviation of the final conversion.

diffusion. Therefore, autoacceleration occurs. Reaction then slows because the accessibility of free radicals to functional groups is diminished as more chains and cross-links are built to make denser networks. More radicals become trapped in the regions where there are no neighboring functional groups. Finally, the reaction is stopped when no more active radicals are present and all the initiators, except the last one, have decomposed—the system has reached the final conversion.

When the initiation rate constant is raised, the polymerization rate rises in most reaction periods (Figure 4a) because of the higher population of active radicals. However, the final conversion drops. It reaches as low as 0.45 ± 0.007 when $k_I = \infty$. This lowered final conversion at a higher initiation rate constant is due to more severe termination of active radicals, which lowers average kinetic chain length.

The kinetic chain length is the number of propagation steps carried by a free radical. The (cumulative) average kinetic chain length $\bar{\nu}$ can be calculated by

$$\bar{\nu} = \frac{x n_{m0}}{n_{rg}} \tag{2}$$

where x is the conversion of functional groups, n_{m0} is the initial number of functional groups, and n_{rg} is the total number of radicals generated (including the recombined primary radicals that cannot find two reactive neighbors to become chain initiating radicals). According to eq 2, at a fixed initiator concentration, the total amount of free radicals generated at the end of reaction is fixed. (The kinetic chain length of the recombined primary radicals can be considered as zero.) Therefore, the higher the average kinetic chain length, the higher the final conversion.

The effect of the initiation rate constant on the kinetic chain length is shown schematically in Figure 5. A kinetic chain starts its growth at a chain initiating radical site. The growth can be either linear when the radical propagates with a neighboring monomeric functional group or nonlinear when the radical propagates with a neighboring pendant functional group to form a primary cycle, a secondary cycle, or a cross-link. Two kinetic chains can be connected together through cross-linking or radical termination. Moreover, they can also be connected by multiple connections through secondary cyclization. The growth of each kinetic chain stops when the radical is terminated or trapped. As polymerization proceeds, more kinetic chains form because more free radicals are generated. The percolation threshold is reached when a large polymer cluster (percolating network), most likely consisting of different kinetic chains, spans from one side of the lattice to the other side. At high conversions, most kinetic chains are connected together. As the initiation rate constant is raised, more and shorter kinetic chains are formed. This is caused by more free radicals generated and the enhanced termination.

Figure 6 shows the average kinetic chain length during polymerization in the three-dimensional simulations. At a finite initiation rate constant, the average kinetic chain length rises with conversion first, reaches a maximum, and then starts to drop. (With the instantaneous initiation, it monotonically increases as the kinetic chains, all born at the beginning of the reaction, grow longer.) The rise of the average kinetic chain length at low conversions is mainly caused by that termination is limited through reaction−diffusion and that trapping is not yet severe. When the average kinetic chain length passes the maximum, trapping of radicals becomes severe. Thereafter, the average kinetic chain length drops.

Consistent with the snapshot illustration, the average kinetic chain length shortens as the initiation rate constant is raised. The shortened average kinetic chain length is in accord with the observation that the dimensionless time, which determines the number of initiators decomposed, rises with the initiation rate constant at a given conversion (Figure 4b). Furthermore, experimental observation of the average kinetic chain length measured by using matrix-assisted laser desorption/ionization time-of-flight mass spectrometry (MALDI−TOF MS)[25] agrees with this trend. At 0.7 conversion of double bonds in the polymerization of difunctional anhydride, the average kinetic chain length drops from 23 to 14 as light intensity is raised from 10 to 100 mW/cm^2 (which is equivalent to raising k_I from 0.0045 to 0.045 1/s). The short average kinetic chain length measured is due to chain transfer in the system.

The final conversion is different from the "final" conversion observed in experiments. The latter is generally determined when the reaction rate drops to a certain fraction (e.g., 1% or 0.1%) of the maximum reaction rate;[1] thus, it is not a real final conversion, and the amount of initiators decomposed can vary significantly. It is generally observed that the "final" conver-

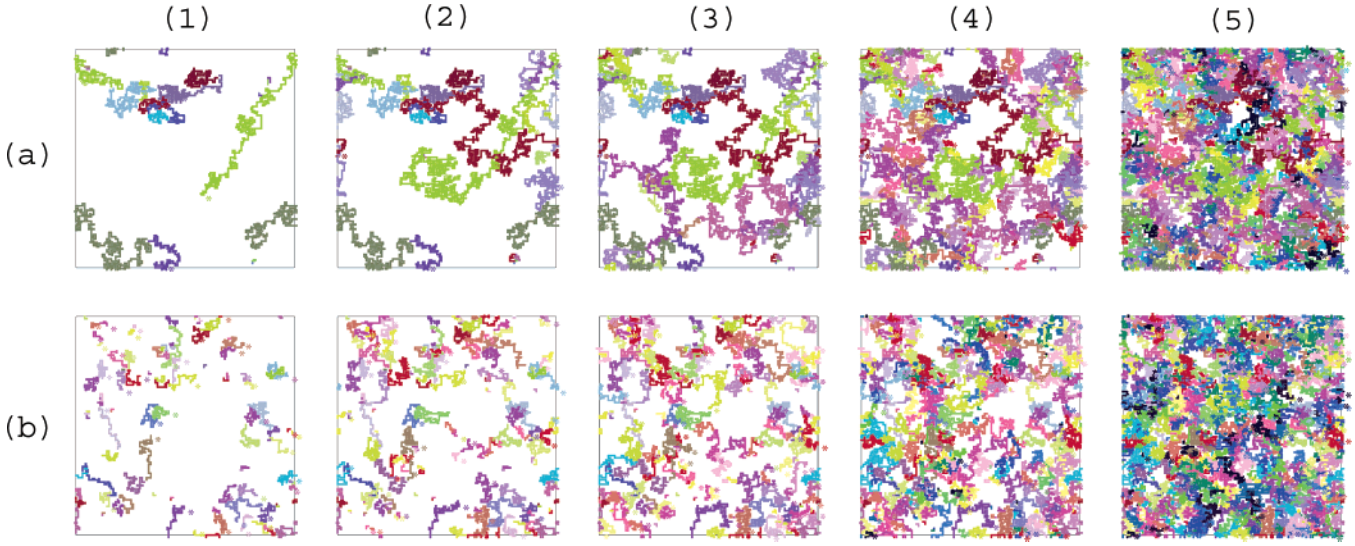

Figure 5. Snapshots of kinetic chains generated by two-dimensional square lattice (100 × 100) simulations with 5% initiator at different conversions of functional groups, (1) 0.1, (2) 0.2, (3) 0.31, (4) 0.5, and (5) 0.75, and two different initiation rate constants, (a) 0.1 1/s and (b) 10 1/s. Percolation threshold occurs at (a2) and (b3). Kinetic chains are identified by different colors. Here only bonds and radicals are shown. A thin line was used to represent one bond formed between two lattice sites, a thicker line represents two bonds formed, and the thickest line represents three bonds formed. Each radical is represented by an asterisk.

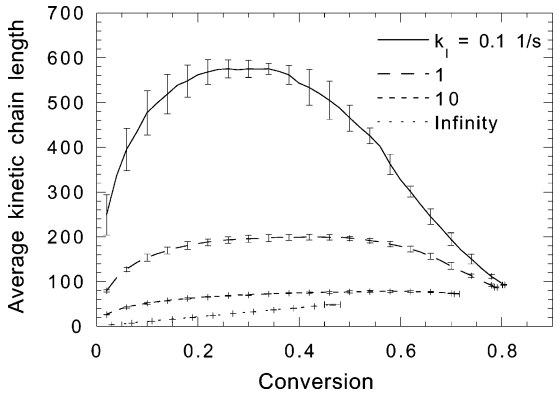

Figure 6. Effect of initiation rate constant k_I on the average kinetic chain length during polymerization. The vertical range bars of every other points are shown, which indicate plus or minus one standard deviation at a given conversion. At the end of each curve, the conversion is the mean final conversion, and the horizontal range bars there indicate plus or minus one standard deviation of the final conversion.

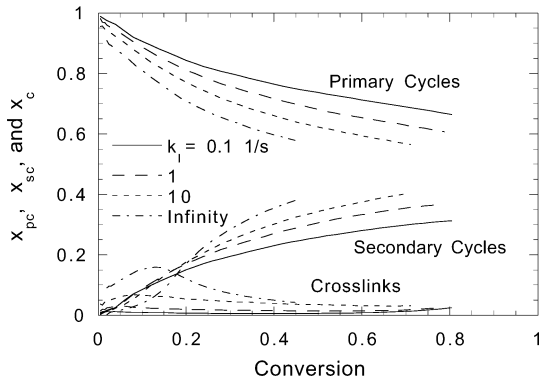

Figure 7. Effect of initiation rate constant k_I on the fractions of the reacted pendant functional groups in primary cycles x_{pc}, secondary cycles x_{sc}, and cross-links x_c vs conversion of functional groups.

sion rises with light intensity in photopolymerization.[1,26] This is caused by the delayed volume shrinkage, which leads to the formation of more excess free volume and with it higher mobilities of functional groups and free radicals.[26] However, volume relaxation is absent in the current model. Nevertheless, the average kinetic chain length should always affect the conversion achieved at a certain amount of initiators decomposed or a certain dose of irradiation in photopolymerization. It was found that the polymerization of 1,6-hexanediol diacrylate (HDDA) at the same dose with 4 orders of magnitude change of light intensity (0.002−2 mW/cm^2) leads to a slight drop of conversion as the light intensity is raised.[27] This is consistent with the simulation result. In general, the conversion at any point should depend on the total number of initiators decomposed, and the competition between the effect of termination or trapping and the effect of volume relaxation on kinetic chain length. The fractions of the reacted pendant functional groups in primary cycles, secondary cycles, and cross-links may give some insights into how volume relaxation might occur (though this is not incorporated in this work).

The pendant functional groups that have reacted form mainly primary cycles and least cross-links during most of the reaction as shown in Figure 7. As polymerization proceeds, the fraction of primary cycles drops with conversion; the fraction of secondary cycles rises; and the fraction of cross-links reaches a maximum at a low conversion, and then it becomes more or less a constant and can grow a little bit at the end. When the initiation rate constant is raised, the amount of cross-links increases, and the amount of primary cycles drops. The amount of secondary cycles becomes slightly lower at low conversions but becomes bigger at high conversions. At a higher initiation rate constant, the total amount of active radicals rises; thus, there is higher chance of forming cross-links and secondary cycles but less chance of forming primary cycles. The initial lower fraction of secondary cycles is because it is more likely to form cross-links when radical concentration is high. The prediction suggests that a higher initiation rate constant leads to more cross-linked structure at low conversions, which might affect the change of free volume in the system. The trend of the fractions of the reacted pendant functional groups in primary cycles, secondary cycles,

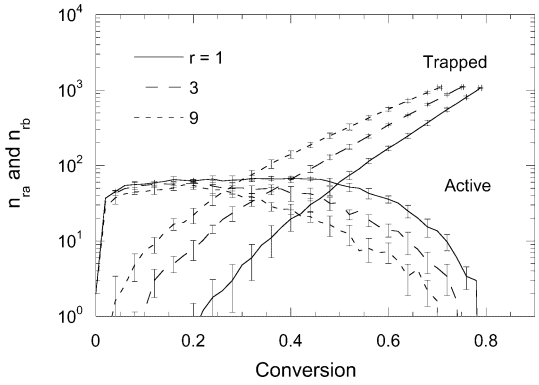

Figure 8. Effect of primary cyclization enhancement factor r on the numbers of active n_{ra} and trapped n_{rb} radicals during polymerization. The vertical range bars of every other points are shown, which indicate plus or minus one standard deviation at a given conversion. At the end of each curve, the conversion is the mean final conversion, and the horizontal range bars there indicate plus or minus one standard deviation of the final conversion.

and cross-links as the initiation rate is varied becomes clearer in the simulations presented here than in previous simulations[28] for three possible reasons: (1) the use of multiple realizations, (2) the calculation of real time, and (3) the use of weighted reaction probabilities.

Effect of Primary Cyclization Enhancement. Figure 8 shows the numbers of active and trapped radicals at different primary cyclization rate constant rk_p, changed by the primary cyclization enhancement factor r. The number of active radicals is not apparently affected by primary cyclization at conversions up to 0.2. At higher conversions though, the number of active radicals drops as the primary cyclization is enhanced. With the enhanced primary cyclization, radical trapping starts at a lower conversion and more radicals become trapped at a given conversion. The more severe the primary cyclization, the higher the fraction of the number of trapped radicals over the total number of radicals (including active and trapped). Also, the crossover of the number of active radicals and the number of trapped radicals moves to a lower conversion, showing that radical trapping starts to dominate earlier. If it is true that monomers with shorter chain length between functional groups tend to form primary cycles more easily due to spatial proximity,[29] the predicted trend here is consistent with ESR observation. Anseth et al. reported that radical trapping started to dominate the total radical population at a lower conversion as monomers change from poly(ethylene glycol)(600) dimethacrylate (PEG600DMA) to poly(ethylene glycol)(200) dimethacrylate (PEG200DMA) and to diethylene glycol dimethacrylate (DEGDMA).[6] When primary cyclization is enhanced, more highly cyclized polymer clusters form, in which higher proportions of functional groups originally present have been converted. Therefore, if a free radical is created in one of these clusters or manages to propagate in, it is less likely to have a reactive neighbor. Consequently, trapping of radicals becomes severe. Furthermore, it has been found in part 1 that the enhanced primary cyclization leads to a less homogeneous network structure at a given conversion.[21] The higher fraction of trapped radicals predicted here suggests again that when radical trapping starts, propagation is more difficult in a less homogeneous structure.

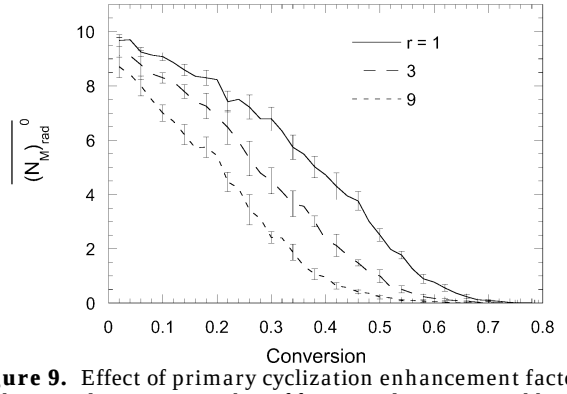

Figure 9. Effect of primary cyclization enhancement factor r on the actual average number of functional groups neighboring each radical $\overline{(N_M)^0_{rad}}$. The vertical range bars of every other points are shown, which indicate plus or minus one standard deviation at a given conversion.

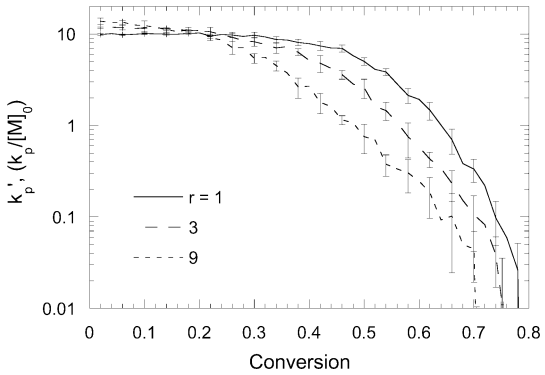

Figure 10. Effect of primary cyclization enhancement factor r on the apparent propagation rate constant k_p'. Range bars of every other points are shown, which are one standard deviation of k_p' at a given conversion.

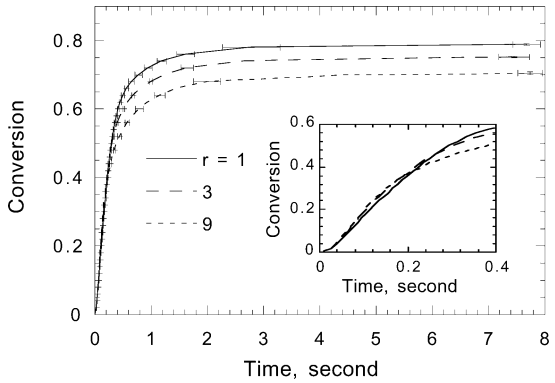

Figure 11. Effect of primary cyclization enhancement factor on the conversion profiles. The horizontal range bars of every other points are shown, which indicate plus or minus one standard deviation at a given conversion. At the end of each curve, the conversion is the mean final conversion, and the vertical range bars there indicate plus or minus one standard deviation of the final conversion.

Figure 9 shows the actual average number of functional groups neighboring each radical $\overline{(N_M)^0_{rad}}$. Starting from very low conversions, $\overline{(N_M)^0_{rad}}$ is severely lowered when the primary cyclization is enhanced. This is again caused by the formation of more highly cyclized clusters. This also indicates that primary cyclization severely lowers the accessibility of free radicals to functional groups and that a less homogeneous structure leads to more difficult propagation.

Figure 10 shows the effect of primary cyclization on the apparent propagation rate constant k_p' during

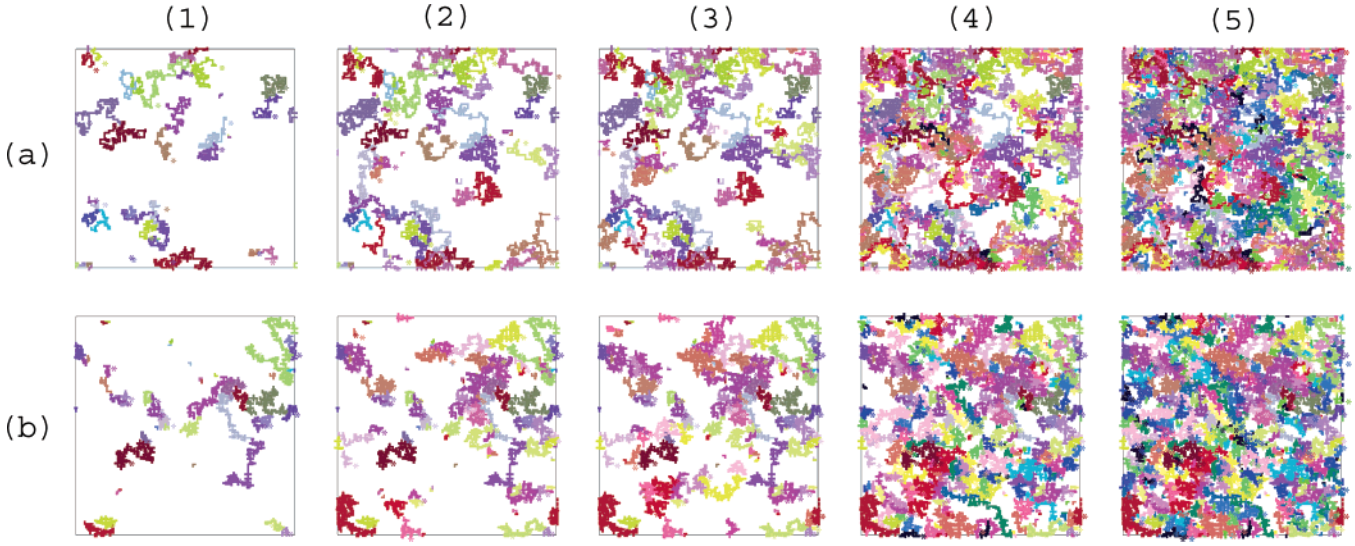

Figure 12. Snapshots of the kinetic chains generated by two-dimensional square lattice (100 × 100) simulations with 5% initiator at different conversions of functional groups, (1) 0.1, (2) 0.23, (3) 0.3, (4) 0.56, and (5) 0.7, and two different primary cyclization enhancement factors, (a) $r = 1$ and (b) $r = 9$. Percolation threshold occurs at (a2) and (b4). Refer to the caption of Figure 5 for snapshot symbols.

reaction. At low conversions, owing to the enhanced primary cyclization and the fact that primary cyclization dominates the reaction of pendant functional groups, k_p' rises with the primary cyclization enhancement factor r. The initial constant k_p' region becomes shorter when the primary cyclization is enhanced, and it almost disappears at $r = 9$. At high conversions, though the pendant functional groups still have a higher reactivity if they can form primary cycles, k_p' drops more severely when the primary cyclization is enhanced. This is due to severe loss of accessibility of free radicals to functional groups. This again indicates that propagation is less favored in a less homogeneous structure. This trend of predicted k_p' agrees with experiment[30] if again monomers with shorter chain length between functional groups tend to form primary cycles more easily. At the beginning of reaction, the measured k_p' is 13.1 and 11.2 in the unit of $k_p/[M_0]$ (assuming the same k_p) in DEGDMA and PEG600DMA, respectively. Moreover, at later stages of reaction, k_p' in the polymerization of DEGDMA drops much faster than PEG600DMA. For instance, at 0.46 conversion, k_p' drops to 1.74 ($k_p/[M_0]$) in the polymerization of DEGDMA, whereas it is still 11.2 ($k_p/[M_0]$) in the polymerization of PEG600DMA.

Figure 11 shows the effect of the primary cyclization enhancement factor on the conversion profiles. Initially, the reaction rate slightly rises when the primary cyclization is enhanced (see the inset in Figure 11) because primary cyclization is the dominant reaction of pendant functional groups at low conversions. After the system reaches about 0.5 conversion, the reaction rate becomes lower when the primary cyclization is enhanced. The final conversion of functional groups also drops. The lowered reaction rate in the later stages of the reaction and the lowered final conversion are caused by more severe radical trapping when the primary cyclization is enhanced. This is the first time to demonstrate that enhanced primary cyclization lowers final conversion. The conversion profiles predicted here also agree with the trend observed[31] in the polymerization of a series of diacrylate monomers with different chain lengths assuming r drops as the chain length is shortened.

The effect of primary cyclization on the kinetic chain length is shown schematically in Figure 12. As the primary cyclization is favored, the kinetic chains are more cyclized (less extended or fewer unreacted pendant functional groups per unit volume). The trends of the amount of kinetic chains and the average kinetic chain length when the primary cyclization is changed are not visible in most of the reaction period via snapshots.

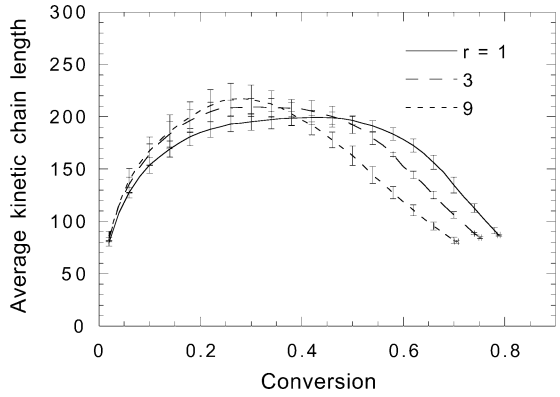

Figure 13. Effect of primary cyclization enhancement factor r on the average kinetic chain length during polymerization. The vertical range bars of every other points are shown, which indicate plus or minus one standard deviation at a given conversion. At the end of each curve, the conversion is the mean final conversion, and the horizontal range bars there indicate plus or minus one standard deviation of the final conversion.

Figure 13 shows the average kinetic chain length in the three-dimensional simulations. The slight increase of the average kinetic chain length at low conversions when the primary cyclization is enhanced is due to the slightly lowered chances of termination. At conversions higher than 0.5, the average kinetic chain length clearly drops when the primary cyclization is enhanced. This is due to more severe radical trapping, which stops the growth of kinetic chains at short lifetime.

The fractions of the reacted pendant functional groups in primary cycles, secondary cycles, and cross-links are shown in Figure 14. When the primary cyclization is enhanced, among the reacted pendant functional groups, the fraction that form primary cycles rises, but the fractions that form secondary cycles and cross-links both drop.

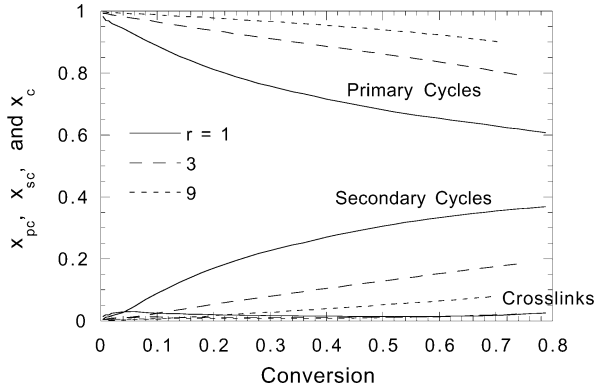

Figure 14. Effect of primary cyclization enhancement factor r on the fraction of the reacted pendant functional groups in primary cycles x_{pc}, secondary cycles x_{sc}, and cross-links x_c vs conversion of functional groups.

The simulation illustrates the importance of primary cyclization on active and trapped radical populations, the accessibility of free radicals to functional groups, the apparent propagation rate constant, conversion profiles, the kinetic chain length, and the formation of different structures by pendant functional groups. This predication has been compared with the polymerization of multifunctional monomers with different chain lengths between functional groups, such as diacrylate and dimethacrylate series. According to available experiment data of radical populations, k_p', and conversion profiles, agreements between the simulation and experiment have been found. This suggests that the tendency of primary cyclization could be an important factor affecting kinetics of these series. In the literature, cross-link density is generally used to explain the experimental data in these series. However, this cross-link density is not specific because at high conversions, it may be hard to distinguish the pendant functional groups that contribute to the primary cycles and the pendant functional groups that contribute to cross-links if the history of kinetic chains is unknown.

Conclusions

The kinetic gelation model presented here uses a realistic reaction time, which allows the rate of generating free radicals to be more accurately counted than previous kinetic gelation models. This model is used to examine the effect of structural inhomogeneity—the spatial distribution of reacted sites—on the populations of active and trapped radicals, the accessibility of free radicals to functional groups, and the apparent propagation rate constant. It is also used to predict the final conversion, the distribution of kinetic chain length, and the fractions of reacted pendant functional groups in primary cycles, secondary cycles, and cross-links.

The predicted apparent propagation rate constant remains truly constant at low conversions, but it then drops by orders of magnitude as free radicals encounter obstacles in accessing functional groups. This trend has been observed in experiment,[7,23,24] and it is hoped that simulations such as those here, done with careful attention to reaction time, might allow the experimentalist to deduce how structural heterogeneity might cause these trends.

In general, the more homogeneous the structure formed at a given conversion (i.e., the more uniformly distributed the reacted sites, such as at a higher initiation rate constant or a lower primary cyclization enhancement factor), the lower the fraction of trapped radicals, the higher the accessibility of free radicals to functional groups, and the higher the apparent propagation rate constant.

The conditions that favor radical trapping or termination (i.e., raising the primary cyclization rate constant or the initiation rate constant) shorten the kinetic chain length and can lower the final conversion (at the point of initiator exhaustion). Some aspects of these trends have been glimpsed in earlier work,[18] but the comprehensive set of simulations allows general trends to be made clear. When comparing final conversions with experiment, though, it is important to note that no polymer motion or excess free volume (from delay of shrinkage) is accounted for in the simulations. Rarely are commercial coatings exhausted of initiator; instead, the "final" experimental conversion is often dictated by the slowing with shrinkage and vitrification. The trend in final conversion presented here would hold at low initiator concentration but should be superseded by a trend (not predicted here) dominated by shrinkage and vitrification.

The kinetic trends reported here can be traced to structural features. For instance, the higher the radical concentration (at a higher initiation rate constant) and the less severe the primary cyclization, the lower the fraction of the reacted pendant functional groups in primary cycles, and the higher the fractions in cross-links and secondary cycles. The structural trends can help the experimentalist to understand and predict apparent rate trends.

Acknowledgment. We acknowledge support from the Center for Interfacial Engineering, a NSF Engineering Research Center at the University of Minnesota, through its Coating Process Fundamentals Program.

References and Notes

(1) Kloosterboer, J. G. *Adv. Polym. Sci.* **1988**, *84*, 1−66.
(2) Pappas, S. P. *Radiation Curing: Science and Technology*; Plenum: New York, 1992.
(3) Decker, C.; Zahouily, K. *Polym. Mater. Sci. Eng.* **1993**, *68*, 70−71.
(4) Fouassier, J.-P., Rabek, J. F., Eds. *Radiation Curing in Polymer Science and Technology*; Elsevier Applied Science: London, 1993; Vol. 4.
(5) Zhu, S.; Tian, Y.; Hamielec, A. E.; Eaton, D. R. *Macromolecules* **1990**, *23*, 1144−1150.
(6) Anseth, K. S.; Anderson, K. J.; Bowman, C. N. *Macromol. Chem. Phys.* **1996**, *197*, 833−848.
(7) Anseth, K. S.; Wang, C. M.; Bowman, C. N. *Macromolecules* **1994**, *27*, 650−655.
(8) Anseth, K. S.; Bowman, C. N. *Polym. React. Eng.* **1993**, *1*, 499−520.
(9) Decker, C.; Moussa, K. *J. Appl. Polym. Sci.* **1987**, *34*, 1603−1618.
(10) Mikos, A.; Takoudis, C.; Peppas, N. A. *Macromolecules* **1986**, *19*, 2174−2182.
(11) Tobita, H.; Hamielec, A. *Makromol. Chem. Makromol. Symp.* **1988**, *20/21*, 501−543.
(12) Tobita, H.; Hamielec, A. *Macromolecules* **1989**, *22*, 3098−3105.
(13) Bowman, C. N.; Peppas, N. A. *Macromolecules* **1991**, *24*, 1914−1920.
(14) Kurdikar, D. L.; Peppas, N. A. *Macromolecules* **1994**, *27*, 4084−4092.
(15) Manneville, P.; de Seze, L. In *Numerical Methods in the Study of Critical Phenomena*; Dora, J. D., Demongeot, J., Lacolle, B., Eds.; Springer-Verlag: Berlin, 1981; pp 116−124.
(16) Boots, H.; Pandey, R. B. *Polym. Bull. (Berlin)* **1984**, *11*, 415−420.
(17) Simon, G. P.; Allen, P. E. E.; Bennett, D. J.; Williams, D. R. G.; Williams, E. H. *Macromolecules* **1989**, *22*, 3555−3561.

(18) Bowman, C. N.; Peppas, N. A. *J. Polym. Sci., Part A: Polym. Chem.* **1991**, *29*, 1575−1583.
(19) Anseth, K. S.; Bowman, C. N. *Chem. Eng. Sci.* **1994**, *49*, 2207−2217.
(20) Chiu, Y. Y.; Lee, L. J. *J. Polym. Sci., Part A* **1995**, *33*, 269−283.
(21) Wen, M.; Scriven, L. E.; McCormick, A. V. *Macromolecules* **2003**, in press.
(22) Gillespie, D. *J. Comput. Phys.* **1976**, *22*, 403−434.
(23) Anseth, K. S.; Wang, C. M.; Bowman, C. N. *Polymer* **1994**, *35*, 3243−3250.
(24) Goodner, M. D.; Bowman, C. N. *Macromolecules* **1999**, *32*, 6552−6559.
(25) Burkoth, A. K.; Anseth, K. S. *Macromolecules* **1999**, *32*, 1438−1444.
(26) Kloosterboer, J. G.; van de Hei, G. M. M.; Dorant, G. C. M. *Polym. Commun.* **1984**, *25*, 322−325.
(27) Kloosterboer, J. G.; Lijten, G. F. C. *Polymer* **1990**, *31*, 95−101.
(28) Anseth, K. S.; Bowman, C. N. *J. Polym. Sci., Part B: Polym. Phys.* **1995**, *33*, 1769−1780.
(29) Kannurpatti, A. R.; Anseth, J. W.; Bowman, C. N. *Polymer* **1998**, *39*, 2507−2513.
(30) Anseth, K. S.; Kline, L. M.; Walker, T. A.; Anderson, K. J.; Bowman, C. N. *Macromolecules* **1995**, *28*, 2491−2499.
(31) Wen, M.; Scriven, L. E.; McCormick, A. V. *Macromolecules* **2002**, *35*, 112−120.

MA010309I